APPLICATION OF GODUNOV-TYPE SCHEMES TO TRANSIENT MIXED FLOWS

Arturo S. León
Post-doctoral Research Associate, V. T. Chow Hydrosystems Lab., Dept. of Civil and Envir. Engng.,Univ. of Illinois at Urbana-Champaign, 2519 Hydrosystems Lab., MC-250. 205 North Mathews Av., Urbana, IL 61801. E-mail: asleon@uiuc.edu (corresponding author).

Mohamed S. Ghidaoui
Professor, Dept. of Civil Engineering, The Hong Kong University of Science and Technology, Room 3569, Clear Water Bay, Kowloon, Hong Kong. E-mail: ghidaoui@ust.hk

Arthur R. Schmidt
Research Assistant Professor, V. T. Chow Hydrosystems Lab., Dept. of Civil and Envir. Engng., Univ. of Illinois at Urbana-Champaign, 2535a Hydrosystems Lab., MC-250. 205 North Mathews Av., Urbana, IL 61801. E-mail: aschmidt@uiuc.edu

Marcelo H. García
Chester and Helen Siess Professor and Director, V. T. Chow Hydrosystems Lab., Dept. of Civil and Envir. Engng., Univ. of Illinois at Urbana-Champaign, 2535b Hydrosystems Lab., MC-250. 205 North Mathews Av., Urbana, IL 61801. E-mail: mhgarcia@uiuc.edu

Abstract

A robust model for simulating the simultaneous occurrence of free surface and pressurized flows is presented using the Preissmann slot approach for modeling pressurized flows. This model is capable of simulating transient flows in closed conduits ranging from free surface flows, to partly free surface-partly pressurized flows (mixed flows), to fully pressurized flows. Its robustness for simulating mixed flows is accomplished by: (1) Introducing a gradual transition between the pipe and the slot, and (2) Using a second-order Godunov-type scheme with a slope limiter to solve the governing free surface flow equations. The accuracy and robustness of the *modified Preissmann model* is investigated using five test cases. The results show that the proposed model accurately describes complex flow features, such as negative open channel-pressurized flow interfaces and interface reversals. The results also show that the proposed model is able to produce stable results for strong (rapid) transients at field scale where no sub-atmospheric flows occur.

Keywords: Open channel flow, Pipe, Pressurized flow, Sewer, Simulation, Transient flow, Unsteady flow

1 Introduction

Although storm-sewer systems are generally designed based on free surface flow, large variations in the inflow and outflow from these systems in practice result in flow conditions that vary from dry to free surface flow, to partly free surface-partly pressurized flow (mixed flow), and to fully pressurized flow. The transition between free surface and pressurized flows is of particular importance because it is often associated with infrastructural damage and problems of operation and control in storm-sewer systems.

The approaches for modeling mixed flows can be divided into two general categories (e.g., Li and McCorquodale 1999, León et al. 2006 b), namely: (1) Simulation of pressurized flows as free surface flow using a hypothetical narrow open-top slot ("Preissmann slot"); and (2) Separate simulation of the free surface and pressurized flows. The hypothetical slot approach is computationally simpler as it only requires

solution for one flow type (free surface flow); however, when using this approach, four main problems associated with the approach itself and with the numerical scheme used to solve the governing equations may be found: First, the inability of the Preissmann slot approach to describe sub-atmospheric full-pipe flows; Second, mass and momentum balance problems associated with the width of the slot; Third, instability problems associated with the poor performance of the numerical scheme when the flow changes rapidly from the pipe to the slot; and Fourth, inaccuracies in the propagation of pressurized transients (flow in slot) associated with the width of the slot.

The Preissmann approach has been used for modeling smooth (gradual) transient mixed flows with good success and strong (rapid) transient mixed flows with poor or no success (e.g., Trajkovic et al. 1999, Yen 2001). The poor success in modeling strong transient flows is mainly due to instability problems when the flow changes rapidly from the pipe to the slot, which may cause the computer simulation to abort. Instability problems are reported even when a slot width as large as 10% of the pipe diameter (e.g., Trajkovic et al. 1999) is used. Artificially wide slots may compromise the accuracy of the simulation if pressurized transients are simulated besides that they may produce mass and momentum balance problems.

The separate simulation of free surface and pressurized flows is more complex; however, the models based on this approach are able to simulate sub-atmospheric pressures in the pressurized flow regime. Current models based on this approach cannot address some complex flow features well, such as open channel surges, negative open channel-pressurized flow interfaces and interface reversals. In this approach, the moving interface that separates the free surface and pressurized flow is tracked and treated as an internal interface. This approach is often referred to as the "shock-fitting" method (e.g., Guo and Song 1990, Fuamba 2002).

Recently, Vasconcelos et al. (2006) introduced a Decoupled Pressure Approach, which is formulated by modifying the open channel Saint-Venant equations to allow for over-pressurization, assuming that the elastic behavior of the pipe walls account for the gain in pipe storage. One of the limitations of this approach is the presence of what these authors call "post shock oscillations" near open channel-pressurized flow interfaces. To keep these oscillations small, lower values for the pressure wave celerity may be used, but this may compromise the accuracy of the simulation if pressurized transients are simulated.

Regardless of the approach used to handle mixed flows, most of the models developed primarily to examine the formation and propagation of hydraulic transients in storm-sewer systems are based on the Method of Characteristics (MOC), usually, the fixed-grid MOC scheme with space-line interpolation (e.g., Cardle 1984, Cardle and Song 1988). León et al. (2006 a) have shown that when this scheme is used to solve the 1D free-surface flow continuity and momentum equations, mass is not conserved and the wave speeds are inaccurate. Accurate prediction of wave speeds is important because these dictate the timing at which surcharging occurs. These authors also show that, for a given level of accuracy, second-order finite volume Godunov-Type Schemes (GTS) require much less execution time than the first-order fixed-grid MOC scheme with space-line interpolation. GTS belong to the family of shock-capturing schemes. These methods capture discontinuities in the solution automatically, without explicitly tracking them (LeVeque 2002). Discontinuities must then be smeared over one or more grid cells. Success requires that the method implicitly incorporates the correct jump conditions, reduces smearing to a minimum, and does not introduce nonphysical oscillations near the discontinuities.

The main aim of this paper is to provide a robust model for simulating transient mixed flows that uses the Preissmann slot approach for the treatment of pressurized flows. The present paper is an extension of a previous work of the same authors (León et al. 2006 a), which was formulated for simulating free surface flows in storm-sewer systems. Herein, a gradual transition between the pipe and the slot is introduced and the governing free surface flow equations are solved using a second-order finite volume GTS scheme with a slope limiter, referred to as the *modified Preissmann model*.

The paper is organized as follows: (1) the governing equations in conservative form for one-dimensional free surface flows are presented; (2) the Finite Volume (FV) discretization of the governing equations is given; (3) one Riemann solver for the flux computation is presented; (4) a brief overview for the formulation of boundary conditions is presented; and (5) the model is tested using five test cases ranging from laboratory experiments to hypothetical tests. Finally, the results are summarized.

2 Governing equations

The one-dimensional open-channel flow continuity and momentum equations for prismatic conduits may be written in their vector conservative form as

$$\frac{\partial \mathbf{U}}{\partial t} + \frac{\partial \mathbf{F}}{\partial x} = \mathbf{S} \tag{1}$$

where the vector variable **U**, the flux vector **F** and the source term vector **S** may be written as (e.g. Guinot 2003, León et al. 2006 a)

$$\mathbf{U} = \begin{bmatrix} A \\ Q \end{bmatrix} \quad \mathbf{F} = \begin{bmatrix} Q \\ \dfrac{Q^2}{A} + \dfrac{A\overline{p}}{\rho} \end{bmatrix} \quad \text{and} \quad \mathbf{S} = \begin{bmatrix} 0 \\ g(S_o - S_f)gA \end{bmatrix} \tag{2}$$

where A = cross-sectional flow area; Q = discharge; $\overline{p}$ = average pressure of the water column over the cross sectional area; ρ = constant liquid density (incompressible flow); g = gravitational acceleration; S_o = slope of bottom channel; and S_f = slope of energy line. The approach proposed herein is applicable to any prismatic conduit, however, only a circular cross-section conduit is considered below.

The Preissmann slot approach is used for the treatment of pressurized flows. As discussed in the Introduction, four main problems are associated with the Preissmann slot approach and with the numerical scheme used to solve the governing free surface flow equations. When using this approach nothing can be done to address the first problem (inability to describe sub-atmospheric full-pipe flows), however the last three problems can be minimized. To address the second problem (mass and momentum balance), a narrow slot can be used. The third problem (instability) is important in modeling strong (rapid) transient flows when the flow changes rapidly from the pipe to the slot, which may cause the computer simulation to abort. To address the fourth problem, a slot width that achieves a gravity wave speed in the slot equal to the water hammer wave speed can be used. This slot width T_s is given by

$$T_s = \frac{gA_f}{a^2} \tag{3}$$

where A_f is the full cross-sectional area of the pipe and a is the water hammer wave speed.

In the *modified Preissmann model*, the fourth problem is addressed by using a slot width that achieves a gravity wave speed in the slot equal to the water hammer wave speed (Eq. 3). This results in a narrow slot, minimizing mass and momentum balance problems (second problem). The third problem (instability) is addressed by (1) using a slope limiter (MINMOD) in the Monotone Upstream-centred Scheme for Conservation Laws (MUSCL)-Hancock method (e.g., Toro 2001) such that the monotonicity of the solution is preserved, and (2) introducing a gradual transition between the pipe and the slot [Fig. 1 (b)] such that the transition between free surface and pressurized flows is gradual.

Differences between results produced by simulations that included and ignored the area of the slot and the pressure force over the slot area were negligibly small. Thus, these parameters were ignored. In the *modified Preissmann model*, for $y < 0.95d$ [Fig. 1 (a)], with d as the diameter of the conduit and y as the water depth, the pressure force over the cross sectional area $A\overline{p}$ is given by

$$A\overline{p} = \frac{\rho g}{12}\left[\left(3d^2 - 4dy + 4y^2\right)\sqrt{y(d-y)} - 3d^2(d-2y)\arctan\frac{\sqrt{y}}{\sqrt{d-y}}\right] \tag{4}$$

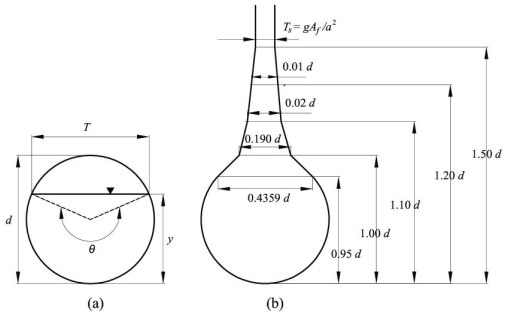

Figure 1 (a) Definition of variables in circular cross sections, (b) Preissmann slot geometry ($y \geq 0.95d$) (not to scale)

3 Formulation of Finite Volume Godunov-type schemes

This method is based on writing the governing equations in integral form over an elementary control volume or cell, hence the general term of Finite Volume (FV) method. The computational grid or cell involves discretization of the spatial domain x into cells of length Δx_i and the temporal domain t into intervals of duration Δt. The ith cell is centered at node i and extends from i–1/2 to i+1/2. The flow variables (A and Q) are defined at the cell centers i and represent their average value within each cell. Fluxes, on the other hand, are evaluated at the interfaces between cells (i–1/2 and i+1/2). For the ith cell, the updating FV formula for the left side of Eq. (1) is given by (e.g., Toro 2001, LeVeque 2002)

$$\mathbf{U}_i^{n+1} = \mathbf{U}_i^n - \frac{\Delta t}{\Delta x_i}\left(\mathbf{F}_{i+1/2}^n - \mathbf{F}_{i-1/2}^n\right) \tag{5}$$

where the superscripts n and n+1 reflect the t and $t+\Delta t$ time levels respectively. In Eq. (5), the determination of $\mathbf{U}$ at the new time step n+1 requires computation of the numerical flux ($\mathbf{F}$) at the cell interfaces at the old time n. To introduce the source terms (right side of Eq. 1) into the solution, a time splitting method using a second-order Runge-Kutta discretization is used (e.g., Zhao and Ghidaoui 2004, León et al. 2006 a). In the Godunov approach, the flux $\mathbf{F}_{i+1/2}^n$ is obtained by solving the Riemann problem with constant states $\mathbf{U}_i^n$ and $\mathbf{U}_{i+1}^n$. This way of computing the flux leads to first-order accuracy of the numerical solution. To achieve second-order accuracy in space and time, the MUSCL - Hancock method (e.g., Toro 2001) is used herein. Second or higher order schemes are prone to spurious oscillations in the vicinity of discontinuities. To preserve the accuracy of the solution away from discontinuities, while ensuring that the solution is oscillation-free near shock waves and other sharp flow features, Total Variation Diminishing (TVD) methods may be used. The TVD property of the MUSCL - Hancock method is ensured by applying the MINMOD pre-processing slope limiter (Toro 2001).

In the Godunov approach, the numerical flux is determined by solving the Riemann problem at each cell interface. Herein, the numerical flux is computed using the HLL (Harten, Lax and Van Leer) Riemann solver. In this approach, the Riemann problem is approximated by an intermediate region $\mathbf{U}_*$ (star region) of constant state separated from the left and right states $\mathbf{U}_L$ and $\mathbf{U}_R$ by two waves. The HLL numerical flux is given by (e.g., Toro 2001, LeVeque 2002)

$$\mathbf{F}_{i+1/2} = \begin{cases} \mathbf{F}_L & \text{if } s_L > 0 \\ \mathbf{F}_* = \dfrac{s_R\mathbf{F}_L - s_L\mathbf{F}_R + s_R s_L\left(\mathbf{U}_R - \mathbf{U}_L\right)}{s_R - s_L} & \text{if } s_L \leq 0 \leq s_R \\ \mathbf{F}_R & \text{if } s_R < 0 \end{cases} \tag{6}$$

where s_L and s_R are the wave speed estimates for the left and right states, respectively. To determine which flux condition to use in Eq. (6), the wave speeds s_L and s_R need to be determined. There are several possible

choices for the wave speed estimates. Toro (2001) proposed a choice of wave speeds for rectangular channels that leads to accurate and robust schemes. León et al. (2006 a) extended these estimates for an arbitrary cross-section channel that can be used for circular cross-section channels including the Preissmann slot region. These wave speed estimates were used in this paper and are given by

$$s_L = u_L - \Omega_L, s_R = u_R + \Omega_R \tag{7}$$

where Ω_K ($K = L, R$) is given by

$$\Omega_K = \begin{cases} \sqrt{\frac{(h_* - h_K)A_*}{\rho A_K (A_* - A_K)}} & \text{if } A_* > A_K \\ c_K & \text{if } A_* \le A_K \end{cases} \tag{8}$$

where c is the gravity wave celerity and $\eta = A\bar{p}$. In Eq. (8), A_* and η_* are unknowns, however, η_* is a function of A_* or vice versa. Thus, only one variable (A_* or η_*) is needed to estimate Ω_K. In Appendix A, several estimates for A_* are provided. In presence of wet-dry interfaces, the HLL approach also offers a simple way for computing the numerical fluxes. In this case, the wave speeds s_L and s_R can be determined exactly (Appendix B).

In the *modified Preissmann model*, when $0 \le min(y_L, y_R) < d/1000$, a wet-dry interface is assumed to be present. In this case, the wave speeds s_L and s_R are computed using the equations provided in Appendix B. Otherwise, the wave speeds are computed using Eq. (7). In the latter, an estimate for A_* is needed for the waves speeds to be fully determined. In the proposed model, the estimate for A_* is based on the depth positivity condition Riemann solver for $max(y_L, y_R) < 0.80d$ and on the two-rarefaction wave approximation for $max(y_L, y_R) \ge 0.80d$.

4 Boundary conditions

Herein, a single set of governing equations (free surface flow) is used for modeling free surface and pressurized flows. Thus, the boundary conditions used are equivalent to those used in free surface flows. In the Godunov approach, for the order of accuracy of the numerical solution to be preserved, it is necessary to use the same order of reconstruction of the flow variables in all the cells. Since common procedures of reconstruction such as MUSCL use one or more cells on each side of the cell to be reconstructed, generally one or more cells are missing within the first and last cells of the computational domain. Herein, second-order accurate boundary conditions are implemented using ghost cells outside of the boundaries (see e.g. LeVeque 2002, León et al. 2007).

In a typical storm-sewer system, various types of boundaries are present. These may include drop shafts, reservoirs, junctions, dead ends, control gates, or pumping stations. Due to space limitations, only a three-way junction boundary is described here. However, several boundaries are special cases of the three-way junction boundary. For instance, a drop shaft boundary is a special case of the three-way junction boundary with no inflow pipes. A downstream reservoir boundary also is a special case of the three-way junction boundary with one inflow pipe, no outflow pipe, and a large drop shaft area.

In a three-way junction boundary (Fig. 2), seven variables are unknown, namely, the flow depth and the flow velocity at each pipe boundary, and the flow depth at the drop shaft pond. Thus, seven equations are needed to determine the unknown variables. The three first equations are obtained by applying the Rankine-Hugoniot conditions between each pipe boundary and the first cell of the corresponding pipe adjacent to the drop shaft. This formulation is intrinsically conservative (mass and momentum are conserved), and no special treatment in presence of shocks at the boundary is required. This yields

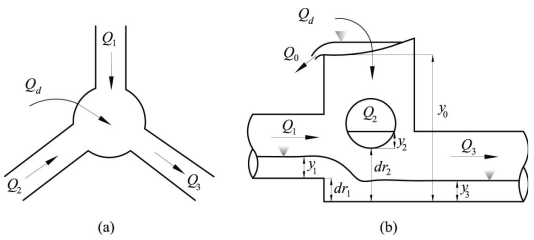

Figure 2 Schematic of reservoir junction with overflow structure (a) Plan view, (b) Side view

$$\left(u_{b_1}^{n+1} - u_1^n\right)^2 - \frac{\left(h_{b_1}^{n+1} - h_1^n\right)}{r}\frac{\left(A_{b_1}^{n+1} - A_1^n\right)}{A_{b_1}^{n+1}A_1^n} = 0 \tag{9}$$

$$\left(u_{b_2}^{n+1} - u_2^n\right)^2 - \frac{\left(h_{b_2}^{n+1} - h_2^n\right)}{r}\frac{\left(A_{b_2}^{n+1} - A_2^n\right)}{A_{b_2}^{n+1}A_2^n} = 0 \tag{10}$$

$$\left(u_{b_3}^{n+1} - u_3^n\right)^2 - \frac{\left(h_{b_3}^{n+1} - h_3^n\right)}{r}\frac{\left(A_{b_3}^{n+1} - A_3^n\right)}{A_{b_3}^{n+1}A_3^n} = 0 \tag{11}$$

where the subscript b_k ($b_k = b_1$, b_2 and b_3) refers to the pipe boundary, and subscript j (j = 1, 2 and 3) to the corresponding adjacent cell to the boundary.

When the flow at the junction changes smoothly and no shocks are present, the theory of Riemann invariants (León et al. 2006 a) is preferred instead of the Rankine-Hugoniot conditions for numerical stability reasons. The fourth equation is obtained from the mass balance at the drop shaft

$$\frac{\left(Q_d^{n+1} + Q_d^n\right)}{2} - \frac{\left(Q_0^{n+1} + Q_0^n\right)}{2} + \frac{\left(Q_{b_1}^{n+1} + Q_{b_1}^n\right)}{2} + \frac{\left(Q_{b_2}^{n+1} + Q_{b_2}^n\right)}{2} - \frac{\left(Q_{b_3}^{n+1} + Q_{b_3}^n\right)}{2} = A_d \frac{\mathrm{d}E_3}{\mathrm{d}t} \tag{12}$$

where Q_d is the discharge entering the drop shaft (Fig. 2), Q_0 is the overflow discharge, and E_3 is the specific energy of the outflow. If the drop shaft has a relatively small storage capacity in comparison to the flow, the right-side of Eq. (12) can be omitted. The specific energy of the outflow is given by

$$E_3 = y_3 + \frac{u_{b_3}^2}{2g} \tag{13}$$

The overflow discharge can be estimated as follows: $Q_0 = 0$, if $y_d \le y_0$, and $Q_0 = CB(y_d - y_0)^{3/2}$, if $y_d > y_0$, in which y_d = flow depth above drop shaft bottom, C = weir discharge coefficient, and B = weir length.

The fifth and sixth equations are obtained by replacing the energy equations by the "kinematic compatibility condition" for the depths (e.g., Pagliara and Yen 1997, Yen 1986, 2001)

For subcritical flow

$$\begin{aligned} y_j &= y_{c_j} && \text{if } dr_j + y_{c_j} > y_3 \\ dr_j + y_j &= y_3 && \text{otherwise} \end{aligned} \tag{14}$$

for $j = 1, 2$, where y_{c_j} *i*s the critical depth.

For supercritical flow

$$\begin{aligned} y_j &= y_{u_j} && \text{if } dr_j + y_{u_j} > y_3 \\ dr_j + y_j &= y_3 && \text{otherwise} \end{aligned} \tag{15}$$

for $j = 1, 2$, where y_{u_j} is the uniform flow depth corresponding to the instantaneous Q_j. The seventh equation is obtained by applying the energy equation between the drop shaft and the outflow pipe (pipe 3). This yields with the loss coefficient K_u

$$y_d^{n+1} = y_{b_3}^{n+1} + \frac{u_{b_3}^2}{2g} + K_u \frac{u_{b_3}\left|u_{b_3}\right|}{2g} \tag{16}$$

5 Evaluation of model

The purpose of this section is to evaluate the accuracy and robustness of the *modified Preissmann model* for simulating strong transient mixed flows in storm-sewers under conditions where no sub-atmospheric flows occur. The ability of the proposed model in simulating pure pressurized flows is also tested. Five test cases are considered, namely:

(1) Experiments type A of Tajkovic et al. (1999),
(2) Experiments type D of Tajkovic et al. (1999),
(3) Trial J of Cardle (1984),
(4) Hypothetical positive shock interface, and
(5) Pressurized flow transients.

5.1 *Experiments type A of Trajkovic et al.* (1999)

In this and the next test case, the proposed model is used to reproduce a set of experiments conducted at the Hydraulics Laboratory of University of Calabria by Trajkovic et al. (1999). The experimental setup consisted of a perspex pipe about 10 m long, having an inner diameter of 10 cm and a Manning roughness coefficient (n_m) of 0.008 $m^{1/6}$. For an explanation of why the units of n_m is $m^{1/6}$ see Yen (1991). Upstream and downstream tanks were connected to the pipe with automatic sluice gates. The experimental investigations evaluated the effect of rapid changes in the opening or closing of the sluice gates. Acknowledging the possible interference of the air phase in case the pipe became pressurized, several vents were placed at the top of the pipe.

In this first test case, the type A set of experiments of Trajkovic et al. (1999) is considered. The initial conditions for this set of experiments were a constant inflow discharge of 0.0013 m^3/s, a bed slope of 2.7%, the upstream sluice gate opening of e_1 = 0.014 m, and the downstream sluice gate totally opened. The transient flow was generated after a rapid (but not instantaneous) closure of the downstream sluice gate that caused the formation of a filling bore moving upstream. After 30 seconds of the gate closure, the gate was partially reopened, producing another transient phenomena. Different values for the re-opening (e_2) were tested. In this test case, three values for the reopening are considered, namely e_2 = 0.008 m, e_2 = 0.015 m, and e_2 = 0.028 m. Simulated and measured pressure traces in sections P3 and P7 for the three re-openings are shown in Fig. 3. The sections P3 and P7 were located 4.6 m and 0.6 m upstream from the downstream sluice gate, respectively. The simulated pressure traces were generated using 100 cells and a maximum Courant number Cr = 0.40.

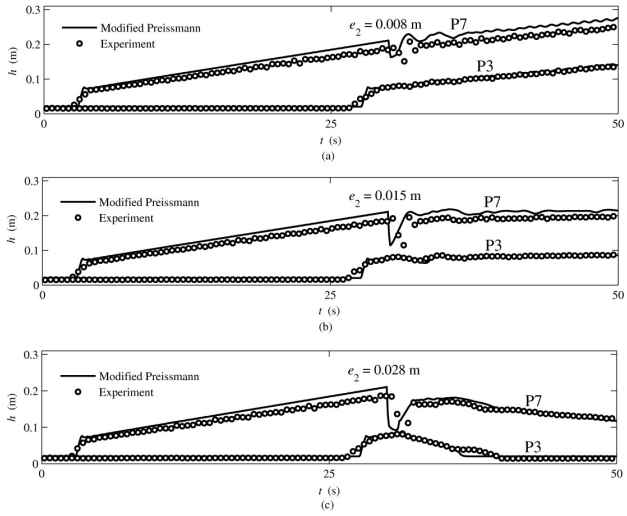

Figure 3 Measured and computer piezometric levels $h(t)$ in sections P3 and P7 for three different downstream valve re-openings e_2

As can be observed from Fig. 3, the simulated pressure head traces $h(t)$ agree well with the corresponding experiments. In particular, the formation of the filling bore and its velocity of propagation are accurately predicted by the *modified Preissmann model*. However, all the computed shock fronts are steeper than the measured. This is because in the experiments the closing of the gate was very rapid, but not instantaneous, as assumed in the simulations. The instantaneous gate closure assumption in the simulations also caused slightly higher pressure heads as compared to the experimental results.

As is shown in Fig. 3, almost immediately after the re-opening of the downstream gate (t = 30 s), a small drop in the pressure head was observed and computed. For a reopening of 0.008 m [Fig. 3 (a)], after a small drop in the pressure head, the pressure head continuously increased in all sections. This is because the outflow from the pipe was smaller than the inflow. For a re-opening of 0.015 m [Fig. 3 (b)], a stationary hydraulic jump was observed and computed in the pipe after the drop in the pressure head. For a re-opening of 0.028 m [Fig. 3 (c)], the hydraulic jump traveled downstream, because the outflow was larger than the inflow.

It is interesting to note that Trajkovic et al. (1999), using the Preissmann slot approach and solving the governing equations utilizing a shock capturing scheme, as used herein, reported numerical instabilities in their simulations when the re-opening was 0.015 m or larger. Numerical instabilities were reported even though the slot width they used was as large as 10% of the pipe diameter. Artificially wide slots may spoil the accuracy of the simulation if pressurized transients are simulated besides that they may produce mass and momentum balance problems. In the *modified Preissmann model*, the slot width, above the transition between the pipe and the slot, is chosen so that the gravity wave speed in the slot is equal to the water hammer wave speed. No stability problems were observed when using the *modified Preissmann model*. The most important differences between the proposed model and that of Trajkovic et al. (1999) are: (1) In the proposed model, a slope limiter (MINMOD) is used to preserve the monotonicity of the solution and to control oscillations that may be present around open channel-pressurized flow shock interfaces, unlike the Trajkovic model, and (2) A gradual transition between the pipe and the slot is introduced in the proposed model, in contrast to the Trajkovic model.

5.2 *Experiments type D of Trajkovic et al.* (1999)

In this test case, one type D experiment of Trajkovic et al. (1999) is considered. The initial conditions for this experiment were a constant inflow discharge of 0.0015 m^3/s, a bed slope of 1.4%, the upstream sluice gate opening of e_1 = 0.015 m, and the initial opening of the downstream sluice gate was 0.033 m. These initial conditions produced a stationary hydraulic jump between sections P6 and P7 of the experiment. Section P6 was located 1.6 m upstream from the downstream sluice gate. The transient phenomena was generated after the downstream gate was rapidly closed at t = 0 and re-opened to its initial position after 16

s. The simulated and measured pressure head traces in section P7 are shown in Fig. 4. The simulated pressure trace was generated using 200 cells and a $Cr = 0.40$.

As can be observed from Fig. 4, the simulated pressure head trace for $t < 16$ s (before the downstream gate was re-opened) is slightly overpredicted. This may be attributed in part to the instantaneous gate closure assumption in the simulations. Furthermore, the initial piezometric levels in the pipe for the simulation of the transient flow were unknown, so it was necessary to generate these computationally. As in the experiment, a stationary hydraulic jump between sections P6 and P7 was obtained computationally with the initial conditions. However, the computed pressure head at section P7 was slightly larger than the measured (compare pressured heads at $t = 0$ in Fig. 4). This fact may have contributed in part to the over-prediction of the computed pressure head before the downstream gate was reopened. After the downstream gate was re-opened, the simulated results agree well with the experiments.

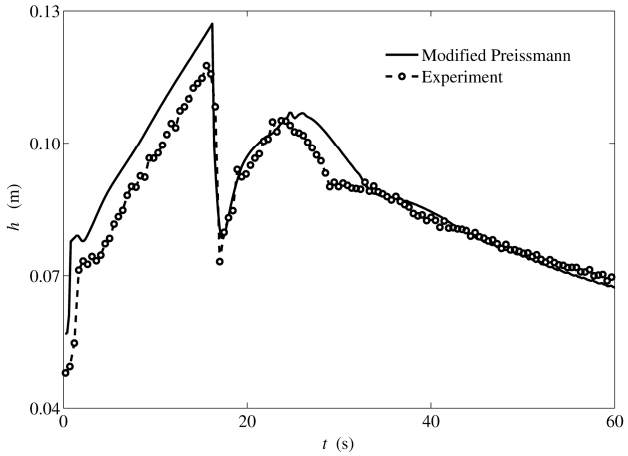

Figure 4 Measured and computed pressure head traces $h(t)$ in section P7 for type D experiment of Trajkovic et al. (1999)

5.3 *Trial J of Cardle* (1984)

In this test case, the ability of the *modified Preissmann model* to simulate a positive shock interface (an interface is defined to be positive when it is moving from the pressurized flow region toward the open channel flow region, and negative otherwise) reversing direction and becoming a negative interface was tested, by comparing the results of the proposed model against experimental measurements conducted at the St. Anthony Falls Laboratory of the University of Minnesota. These experiments were reported in a number of publications including Cardle (1984), which was used herein. The experimental setup consisted of a 48.77 m long clear PVC pipe of inner diameter of 16.26 cm. An upstream head tank and a downstream reservoir were connected to the pipe with automatic sluice gates.

In this test case, the trial J experiment of Cardle (1984) is considered. The initial conditions for this experiment were a constant inflow discharge of 0.005097 m^3/s, a bed slope of 0.05%, and a downstream reservoir depth of 0.1372 m. The Manning roughness value suggested by Cardle (1984) of 0.011 $m^{1/6}$ was used in our simulations. The transient flow was produced after a rapid but not instantaneous closure of the downstream gate creating a positive interface moving upstream. When this interface had advanced about 24.4 m, the gate was instantly re-opened. In the simulations, the re-opening occurred at about 15 s after the gate was closed. After gate re-opening, the positive interface continued to move upstream propelled by its own inertia but after a short time the interface reversed its direction and retreated back downstream. Meanwhile, a negative interface was formed at the downstream boundary and started to move upstream.

The simulated and measured pressure heads at transducer P1, which is located at 9.14 m upstream from the downstream end, are presented in Fig. 5. The simulated pressure trace was generated using 200 cells and a $Cr = 0.50$. As can be observed in Fig. 5, the simulated results agree again well with the experimental measurements. However, the arrival of the simulated positive interface to transducer P1 is slightly earlier as compared to the experiments. This may be because in the experiments the closing of the gate was rapid, but not instantaneous, as was assumed in the simulations. The instantaneous gate closure assumption in the

simulations also caused slightly higher pressure heads as compared to the experiments. The oscillations in the measured pressure heads, after the gate was reopened ($t \approx 15$ s), may be due to the presence of air bubbles near the pipe crown in the experiment.

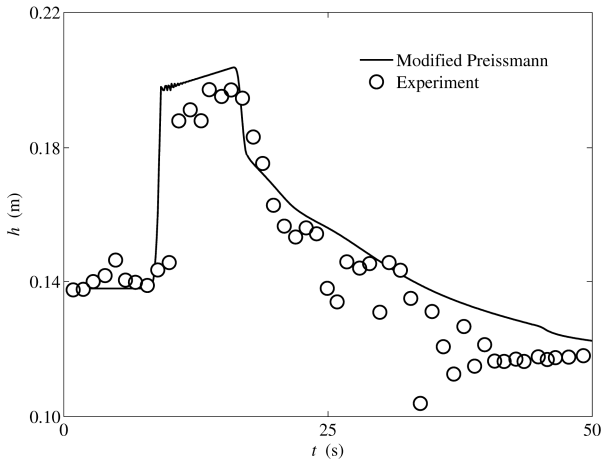

Figure 5 Measured and computed pressure head traces $h(t)$ at transducer P1 for trial J experiment of Cardle (1984)

5.4 *Hypothetical positive shock interface*

The previous test cases investigated the ability of the proposed model in simulating complex flow features including positive shock interfaces. These test cases were laboratory experiments, in which the achieved pressure heads were very small. Since the proposed model is intended to be used in field applications and due to the lack of experimental data in these situations, this test case and the next present hypothetical tests in order to investigate the capability of the proposed model in simulating strong transients at field scale.

The hypothetical test presented below considers a sloped tunnel connected to a downstream valve. The tunnel length is 10,000 m and its diameter is 10 m, the tunnel slope is 0.1%, the Manning's roughness coefficient is 0.015 $m^{1/6}$, the waterhammer wave speed assumed is 1,000 m/s and the initial steady-state discharge is 240 m^3/s, which results in a steady-state flow velocity of 4.3 m/s and an initial normal depth of 6.7 m.

The transient flow is obtained after an instantaneous closure of the downstream valve at time $t = 0$. The gate closure created a strong positive shock interface moving upstream. The simulated pressure heads 300, 600, and 900 s after the gate closure and the "Near exact" solution are shown in Fig. 6. The "Near exact" solution is obtained by grid refinement until convergence is achieved. The simulated pressure heads were obtained using 500 cells and a maximum Courant number of $Cr = 0.5$. As can be observed in Fig. 6, the "Near exact" shock interface is well resolved by the proposed model.

In the *modified Preissmann model*, the slot width is chosen so that the gravity wave speed in the slot is equal to the water hammer wave speed. This results in a slot width of about 0.77 mm (0.0077% d) for the present test case. When using larger slot widths, such as 0.5% d, 1% d and 2% d, the results, though not shown, were similar. This explains why researchers using wide slots (to avoid numerical instability) obtained good agreement with experiments when simulating mixed flows. Artificially wide slots may be used with good accuracy when simulating mixed flows. However, as is shown in the next test case, when simulating pure pressurized flows (flow in slot), only a slot width that is obtained by making the gravity wave speed in the slot equal to the water hammer wave speed gives accurate results for the propagation and magnitude of pressurized transients. Unlike other Preissmann models that report numerical instabilities even when a slot width as large as 10% of the pipe diameter is used, no instabilities were found when using the *modified Preissmann model* (slot width is about 0.0077% d for this test case) even though strong transients at field scale are simulated.

5.5 *Pressurized flow transients*

The purpose of this section is to test the ability of the proposed model in simulating pressurized flow transients. The test considers a horizontal frictionless tunnel connected to an upstream reservoir and a downstream valve. The length of the tunnel is 10,000 m and its diameter is 10 m, the upstream reservoir constant head is h_0 = 200 m, the initial steady-state flow velocity is 2.0 m/s, and the water hammer wave speed is 1000 m/s. The transient flow is obtained after an instantaneous closure of the downstream valve. The simulated pressure heads 3, 6 and 9 s after the gate closure and the "Near exact" solution are shown in Fig. 7. The "Near exact" solution is obtained by grid refinement until convergence is achieved. The simulated pressure heads were obtained using 500 cells and a maximum Courant number of Cr = 0.8.

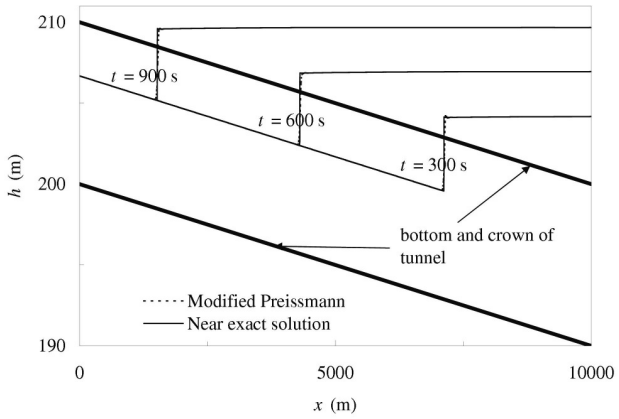

Figure 6 Simulated pressure heads $h(x)$ for strong transient mixed flows

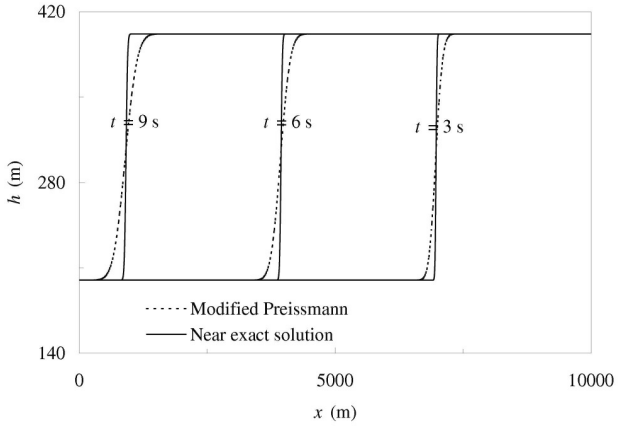

Figure 7 Simulated pressure heads $h(x)$ for pressurized flow transients for a slot width of 0.77 mm

As can be observed from Fig. 7, the "Near exact" pressure head is well resolved by the proposed model. The results presented in Fig. 7 were obtained using a slot width (above the transition between the pipe and the slot) suggested in the proposed model [Eq. (3)], resulting in a slot width of 0.0077% d. Additional simulations were carried out to investigate the influence of using wide slots for simulating the propagation of pressurized transients. The results for a slot width of 1% d together with the "Near exact" solution are presented in Fig. 8. As can be observed, the simulated results using a slot width of 1% d are not even close to the "Near exact" solution. This is because the gravity wave speed for this slot width (87.8 m/s) is much smaller than the water hammer wave speed (1000 m/s). It must be recalled that in pure pressurized flows, the water hammer wave speed determines how fast the pressure transients are propagated. Evidently, the only way of reproducing the correct propagation and interaction of pressurized

transients is by using a slot width that results in a gravity wave speed in the slot equal to the water hammer wave speed.

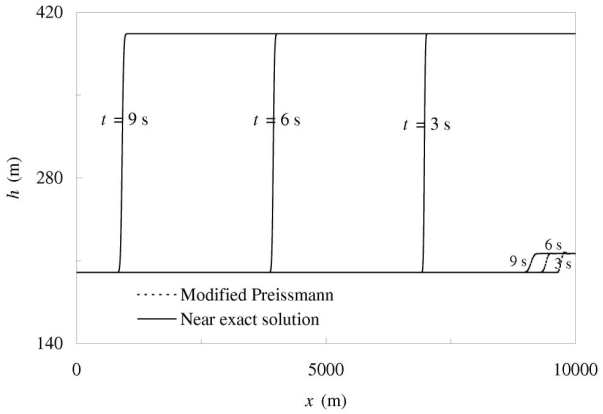

Figure 8 Simulated pressure heads $h(x)$ for pressurized flow transients for a slot width of 1% d

As was mentioned previously, notwithstanding the problems associated with the size of the slot in the Preissmann model, the generic equivalence between the water hammer and the free surface flow equations does not imply that both flows are identical. The use of water level in the Preissmann model to represent the water hammer head prohibits the formation of sub-atmospheric pressures and the emergence of vapor cavities, which would occur in a water hammer flow when the pressure drops below vapor pressure. Whenever the head drops below the slot, the pressure produced by the Preissmann model is equivalent to the water depth in the pipe and the magnitude of the wave speed drops from the water hammer wave speed to the open-channel wave speed. In reality, however, sub-atmospheric water hammer pressures could form during depressurization and the speed of these pressures is equal to the water hammer wave speed. Therefore, Preissmann slot models cannot simulate sub-atmospheric pressures, and the results of these models after, as well as during, depressurization must be treated with caution.

6 Conclusions

The main aim of this research was to provide a robust model for simulating transient mixed flows (where no sub-atmospheric flows occur) in storm-sewer systems using the Preissmann slot approach for the treatment of pressurized flows. In this model, a gradual transition between the pipe and the slot was introduced and the governing equations (free surface flow) were solved using a second-order finite volume GTS scheme with a slope limiter. This model is referred to as the *modified Preissmann model*. Its accuracy and robustness were investigated using five test cases ranging from laboratory experiments to hypothetical tests. The key results of the proposed model are as follows:

(1) It accurately describes complex flow features, such as positive and negative open channel-pressurized flow interfaces, interface reversals and open channel surges,
(2) It is capable of simulating transient flows in closed conduits ranging from free surface flows, to partly free surface-partly pressurized flows (mixed flows), to fully pressurized flows. Pressurized transients are accurately simulated because the slot width, above the transition between the pipe and slot, is chosen in such a way that the gravity wave speed in the slot is equal to the water hammer wave speed,
(3) The formulation of boundary conditions is intrinsically conservative (mass and momentum are conserved at the boundaries) and no special treatment to handle shocks or discontinuities at the boundaries is needed, and
(4) No instability problems were found in the simulations and no simulations aborted during the computations. Overall, the proposed approach is accurate and robust under strong transient flow conditions provided no sub-atmospheric flows occur.

Acknowledgments

The Authors gratefully acknowledge Prof. M. Ivetic and Engineer B. Trajkovic for providing their experimental data in digital format. The Authors also wish to thank the Metropolitan Water Reclamation District of Greater Chicago for their financial support.

Appendix A

Herein, estimates for A_* based on the two-rarefaction wave approximation, the linearization of the governing equations, and the depth positivity condition are provided.

Two-rarefaction wave approximation

Assuming the two-rarefaction wave approximation, the following estimates for the exact solution of A_* (or f_*) and u_* are obtained:

For $y < 0.95d$ (León et al. 2006 a)

$$u_* = \frac{u_L + u_R}{2} + \frac{f_L - f_R}{2} \tag{17}$$

$$f_* = \frac{f_L + f_R}{2} + \frac{u_L - u_R}{2} \tag{18}$$

For $y \geq 0.95d$, the estimates for A_* and u_* are obtained by integrating the differential relationships provided by the generalized Riemann invariants across the two rarefaction waves using the trapezoidal rule. This provides the two following equations that need to be solved by iteration to obtain the estimates of A_* and u_*

$$u_L - u_* + \frac{(c_L + c_*)(A_L - A_*)}{A_L + A_*} = 0 \tag{19}$$

$$u_* - u_R - \frac{(c_* + c_R)(A_* - A_R)}{A_* + A_R} = 0 \tag{20}$$

Linearization of the governing equations

In this approach, A_* is obtained by solving the Riemann problem for the linearized hyperbolic system $\partial \mathbf{U}/\partial t + \overline{\mathbf{A}}\partial \mathbf{U}/\partial x = 0$ with $\overline{\mathbf{A}} = \mathbf{A}(\overline{\mathbf{U}})$ and $\overline{\mathbf{U}} = (\mathbf{U}_L + \mathbf{U}_R)/2$, where $\overline{\mathbf{A}}$ is the Jacobian matrix of the flux vector. This yields with $\overline{A} = (A_R+A_L)/2$ and $\overline{c} = (c_R+c_L)/2$ (León et al. 2006 a)

$$A_* = \overline{A}\left(1 + \frac{u_L - u_R}{2\overline{c}}\right) \tag{21}$$

Unlike in the case of the two-rarefaction wave approximation, in the Riemann solver based on the linearization of the governing equations (Eq. 21) no iteration is required to estimate A_*.

Depth positivity condition

Another estimate for A_* that preserves the simplicity of Eq. (21) while adding two important new properties may be obtained based on the depth positivity condition (flow depth is greater than or equal to zero). The added properties are (Toro 2001): (1) it can handle situations involving very shallow water; and (2) unlike the Riemann solver given in Eq. (21), the Riemann solver based on the depth positivity condition is found

to be very robust in dealing with shock waves. Using this approach, the following estimate for A_* is obtained that is valid for $y < 0.95d$ (León et al. 2006 a)

$$A_* = \frac{A_R + A_L}{2}\left(1 + \frac{u_L - u_R}{f_R + f_L}\right) \tag{22}$$

Appendix B

Below the exact wave speeds s_L and s_R in presence of wet-dry interfaces are presented. In presence of wet-dry interfaces, the governing flow equations are not strictly hyperbolic and the two Eigenvalues of the Jacobian matrix of **F** with respect to **U** collapse into one (e.g., Zoppou and Roberts 2003). Under these circumstances, no shock exists and s_L and s_R represent the speeds of the head or the toe of the rarefaction wave, depending if the dry bed is present upstream ($y_L = 0$) or downstream ($y_R = 0$). In this case, the wave speeds may be determined exactly, yielding for the case of sewers (the derivation of the wave speeds for sewers is similar to the presented by Toro 2001 for a rectangular cross-section)

If $y_L = 0$

$$\begin{aligned} s_L &= u_R - f_R \\ s_R &= u_R + c_R \end{aligned} \tag{23}$$

If $y_R = 0$

$$\begin{aligned} s_L &= u_L - c_L \\ s_R &= u_L + f_L \end{aligned} \tag{24}$$

where c is the gravity wave celerity and f is given by (León et al. 2006 a)

$$f = \sqrt{g\frac{d}{8}}\left(\sqrt{3}q - \frac{\sqrt{3}}{80}q^3 + \frac{19\sqrt{3}}{448000}q^5 + \frac{\sqrt{3}}{10035200}q^7 + \frac{491\sqrt{3}}{27\,´\,7064780800}q^9 + \ldots\right) \tag{25}$$

In the series expansion of Eq. (25), no generic expression for the terms in the series was found.

Notation

A = cross-sectional area of flow
A = Jacobian matrix of flux vector
a = water hammer wave speed
A_d = horizontal cross-sectional area of drop shaft pond
A_f = full cross-sectional area of the pipe
Cr = maximum Courant number
c = gravity wave celerity
d = sewer diameter
E = specific energy
F = flux vector
$\mathbf{F}_{i+1/2}^{n}$ = inter-cell flux at time step n
g = acceleration due to gravity
h = pressure head
K_u = loss coefficient
n_m = Manning roughness coefficient
$\overline{p}$ = average pressure of the water column over cross sectional area
Q = discharge

S = vector containing source terms
S_f = energy line slope
S_o = bed slope
s_L = left wave speed
s_R = right wave speed
T = top width
T_s = slot width
t = time
U = vector of flow variables
$\mathbf{U}_i$ = vector of flow variables at node i
u = water velocity
x = longitudinal coordinate
y = water depth above channel bottom
y_d = water depth above drop shaft bottom
y_0 = distance from drop shaft pond invert to crest of overflow structure
Δx = spatial mesh size
Δt = time step
$\eta = A\overline{p}$
θ = angle of reference
ρ = water density
$f = \int (c / A) \mathrm{d}A$

Superscripts

n = computational time level

Subscripts

i = mesh point location in x-direction
* = star region

References

Cardle, J.A. (1984). An investigation of hydraulic transients in combination free surface and pressurized flows. *Ph.D. thesis*, Dept. of Civil and Mineral Engng., Univ. of Minnesota, Twin Cities, MN.

Cardle, J.A., Song, C.C.S. (1988). Mathematical modeling of unsteady flow in storm sewers. *Int. J. Engng. Fluid Mechanics* 1(4), 495-518.

Fuamba, M. (2002). Contribution on transient flow modeling in storm sewers. *J. Hydr. Research* 40(6), 685-693.

Guinot, V. (2003). *Godunov-type schemes*. Elsevier, Amsterdam NL.

Guo, Q., Song, C.S. (1990). Surging in urban storm drainage systems. *J. Hydr. Engng.* 116(12), 1523-1537.

León, A.S., Ghidaoui, M.S., Schmidt, A.R., García, M.H. (2006 a). Godunov-type solutions for transient flows in sewers. *J. Hydr. Engng.* 132(8), 800-813.

León, A.S., Schmidt, A.R., Ghidaoui, M.S., García, M.H. (2006 b). Review of sewer surcharging phenomena and models. *Civil Engineering Studies, Hydraulic Engineering Series 78*, Univ. of Illinois, Urbana, IL.

León, A.S., Ghidaoui, M.S., Schmidt, A.R., García, M.H. (2007). An efficient second-order accurate shock capturing scheme for modeling one and two-phase water hammer flows. Accepted for publication in J. Hydr. Engng.

LeVeque, R.J. (2002). *Finite volume methods for hyperbolic problems.* Cambridge Press, Cambridge.

Li, J., McCorquodale, A. (1999). Modeling mixed flow in storm sewers. *J. Hydr. Engng*. 125(11), 1170-1180.

Pagliara, S., Yen, B.C. (1997). Sewer network hydraulic model: NISN. *Civil Engng. Studies, Hydr. Engng. Series* 53., Dept. of Civil Engng., Univ. of Illinois at Urbana - Champaign, Urbana, Ill.

Toro, E.F. (2001). *Shock-capturing methods for free-surface shallow flows*. Wiley, Chichester UK.

Trajkovic, B., Ivetic, M., Calomino, F., D'Ippolito, A. (1999). Investigation of transition from free surface to pressurized flow in a circular pipe. *Water Science and Technology* 39(9), 105-112.

Vasconcelos, J.G., Wright, S.J., Roe, P.L. (2006). Improved simulation of flow regime transition in sewers: Two-component pressure approach. *J. Hydr. Engng.* 132(6), 553-562.

Yen, B.C. (1986). Hydraulics of sewers. *Advances in Hydroscience* 14, 1-115. Academic Press, London.

Yen, B.C. (1991). Hydraulic resistance in open channels. *Channel Flow Resistance: Centennial of Manning's Formula*, 1-135. Water Resources Publications, Littleton Co, USA.

Yen, B.C. (2001). Hydraulics of sewer systems. *Stormwater collection systems design handbook*, McGraw-Hill, New York.

Zhao, M., Ghidaoui, M.S. (2004). Godunov-type solutions for water hammer flows. *J. Hydr. Engng.* 130(4), 341-348.

Zoppou, C., Roberts, S. (2003). Explicit schemes for dam-break simulations. *J. Hydr. Engng.* 129(1), 11-34.